



Research Article

A comparison of homogeneous and heterogeneous Brønsted acid catalysts in the reactions of *meso*-erythritol with aldehyde/ketones



Ananda S. Amarasekara¹ · Shahrukh R. Ali¹ · Harshica Fernando¹ · Victoria Sena² · Tatiana V. Timofeeva²

© Springer Nature Switzerland AG 2019

Abstract

Brønsted acid catalyzed condensations of *meso*-erythritol with aldehyde/ketones were studied using *meso*-erythritol:aldehyde/ketone 1:3 ratio in a Dean–Stark apparatus. The selectivity among *bis*-ketal and 1,3-dioxolane-ether formation can be achieved by choosing between homogeneous and heterogeneous catalysts. The catalysts could be reused without appreciable loss in activity.

Keywords *meso*-erythritol · Ketal · Ether · Aldehydes · Ketones · Catalysis

1 Introduction

The acid catalyzed conversion of aldehydes or ketones to their acetals and ketals is a well known reaction in synthetic organic chemistry, widely applied as a protecting technique for carbonyl compounds as well as for 1,2 and 1,3-diols [1]. The acetals and ketals are generally stable under basic and oxidative conditions and can be hydrolyzed under aqueous acidic conditions [1]. The susceptibility of these functionalities to controlled acidic conditions can be seen as an asset in biodegradable polymer applications. The renewed interest in this functionality in recent years may be due to numerous applications like synthesis of biodegradable smart polymer materials [2], oxygenated renewable fuel additives [3] as well as in cosmetics [4]. In recent years a number of researchers have recognized the potential of incorporating the ketal/acetal function in two classes of biodegradable polymers, firstly in environmentally compatible biodegradable polymer materials and secondly in medical applications [5, 6]. For example, Miller and co-workers have shown favorable biodegradation properties in lignin derived ketal polymers

[7, 8]. Furthermore, ketal functionalized chemicals are of interest as new biodegradable surfactants and polymer additives as well; especially levulinic acid ketals as well as esters have attracted interest as eco-friendly surfactants and polymer additives [9, 10]. In medical applications, Shenoi et al. [11] has recently demonstrated that hyper branched polyglycerols with ketal groups are highly biocompatible, with favorable in vivo degradation characteristics with minimal tissue accumulation.

In the case of renewable energy and fuel applications, glycerol ketals/acetals are the most widely studied class of compounds and this may be due to the relative abundance of this natural polyol as a byproduct in the biodiesel industry. The acetone ketal of glycerol, commonly known as solketal has been recognized as a potential replacement for the fuel additive methyl t-butyl ether [3, 12, 13]. In addition numerous researchers have studied the potential of glycerol as a monomer for the renewable carbon based polymer industry. Recently we have shown that condensation of glycerol with renewable monomers such as levulinic, 4-ketopimelic and 2,5-furan dicarboxylic acids can be used to prepare novel renewable polymers

Electronic supplementary material The online version of this article (<https://doi.org/10.1007/s42452-019-0226-9>) contains supplementary material, which is available to authorized users.

✉ Ananda S. Amarasekara, asamarasekara@pvamu.edu | ¹Department of Chemistry, Prairie View A&M University, Prairie View, TX 77446, USA. ²Department of Natural Sciences, New Mexico Highlands University, Las Vegas, NM 87701, USA.

with ketal and ester functionalities [14–16]. However, the higher homolog of glycerol, erythritol has received little attention as a renewable feedstock in the chemical and polymer industry [7, 17, 18].

Since 1990s, erythritol has been produced in an industrial scale and added to beverages and foods to give sweetness, as a flavor enhancer, humectants, formulation support/stabilizer, sequestrant, thickener as well as a texture enhancer. In the US, the main use of erythritol are in chewing gum, baked sweets and in diet beverages [19]. Erythritol can be produced via numerous chemical methods such as halogenations followed by hydrolysis of 2-butene-1,4-diol, hydrogenolysis of tartaric acid esters [20] or dialdehyde starch [21], and electrolytic decarboxylation of arabinoic or ribonic acids [22]. Nevertheless, these chemical synthesis methods are not widely applied in the current industrial production of erythritol as biotechnological methods are more economically feasible and currently most of the erythritol is produced by fermentation methods using yeast-like fungi genera [19, 23]. In addition a number of other common organisms such as: *Moniliella pollinis*, *Trichosporonoides megachiliensis* and *Yarrowia lipolytica* have also been used in the industrial production of erythritol [23].

Erythritol with four hydroxyl groups has the potential of making a symmetrical 1,3-dioxolane *bis*-ketal system, which is more attractive as a polymer building block than glycerol since the triol can make only one ketal/acetal and leaves an unreacted primary alcohol group. However this acid catalyzed *bis*-ketal formation in *meso*-erythritol can get complicated by the possible cyclo-dehydration giving a favorable tetrahydrofuran system. Since there are many Brønsted acid catalysts that can be used in such ketal formation and cyclo-dehydration reactions, it would be interesting to compare different homogeneous and heterogeneous Brønsted acids under similar catalyst loading conditions. The comparison studies of different acid catalysts in a one chemical process is rare in the literature [24, 25] and in one instance Yoon et al. [26] compared the trimerization of isobutene over cation exchange resins and acidic zeolites. In this study they found that zeolites are superior in recyclability in comparison to resin catalysts [26]. In another study Ozbay et al. [24] compared a series of solid acid catalysts including: Amberlyst-15, Amberlyst-16, Amberlyst-35, Amberlyst-36, Lewatit K2629, Relite EXC8D, Nafion SAC-13 and H-Mordenite in the etherification reaction of glycerol using t-butanol. In these experiments Amberlyst-15, with the highest Brønsted acidity, produced the highest yield of glycerol ethers at 90–100 °C. The Brønsted acidity and the rate of diffusion were found to be important properties of the acid catalysts in the glycerol etherification process under the batch reactor conditions used in the experiments [24]. In development of

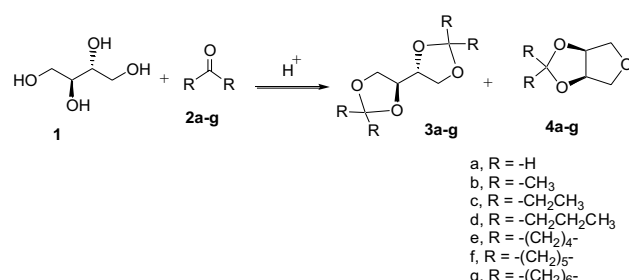


Fig. 1 The *p*-toluenesulfonic acid (*p*-TsOH), 1-(3-propylsulfonic)-3-methylimidazolium chloride [(HSO₃)³C₃C₁im][Cl], Amberlyst-15 H⁺ and sulfonated-silica (SiO₂-SO₃H) catalyzed reactions of *meso*-erythritol (1) with aldehyde/ketones (2a–g)

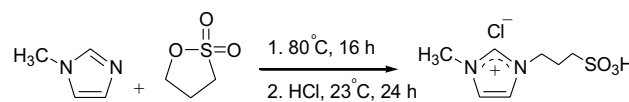


Fig. 2 Synthesis of acidic ionic liquid catalyst, 1-(3-propylsulfonic)-3-methylimidazolium chloride [(HSO₃)³C₃C₁im][Cl] by reaction of 1-methylimidazole with 1,3-propanesultone and acidification [33, 34]

new renewable carbon based ketal functionalized polymer feedstocks we have recently compared the homogeneous and heterogeneous acid catalyzed esterification and ketolization of biomass derived levulinic acid with 1,2-ethane diol and 1,3-propane diol [27]. In these studies we have found that ketals and ketal-esters are formed in Amberlyst-15 catalyzed reactions; while esters and ketal-esters are produced in *p*-toluenesulfonic acid catalyzed reactions [27]. In continuation of our efforts in the development of new biomass derived feedstocks, monomers and polymeric materials [28–32] we have studied the effect of different homogeneous and heterogeneous catalysts on the *bis*-ketal formation as well as in the cyclo-dehydration reactions of *meso*-erythritol as shown in Fig. 1.

2 Results and discussion

The Brønsted acid catalyzed reactions of *meso*-erythritol with a series of aldehyde/ketones were studied by using *p*-toluenesulfonic acid, 1-(3-propylsulfonic)-3-methylimidazolium chloride, Amberlyst-15, sulfonated-silica as catalysts and *meso*-erythritol:aldehyde/ketone 1:3 mol ratio for 24 h. The acidic ionic liquid catalyst, 1-(3-propylsulfonic)-3-methylimidazolium chloride [(HSO₃)³C₃C₁im][Cl] was prepared using our previously reported procedure as shown in Fig. 2 [33, 34]. The products were identified by comparison with published ¹H and ¹³C NMR data [35–39].

A representative ^1H NMR spectrum of the *bis*-ketal (**3b**), ketal-ether (**4b**) product mixture from the Amberlite-15 catalyzed reaction of *meso*-erythritol (**1**), with acetone (**2b**) is shown in Fig. 3.

The preliminary experiments with *meso*-erythritol:aldehyde/ketone 1:2 ratio and shorter reaction times failed to give complete conversion of *meso*-erythritol to ketals or cyclic ether-ketals. Therefore all experiments were carried out with *meso*-erythritol:aldehyde/ketone 1:3 ratio and 24 h, which gave complete conversions and presumably the thermodynamic products. Furthermore, symmetrical aldehyde/ketones were used in the study to stay away from the formation of stereoisomer mixtures. The results of total % yields and mol % compositions in using five aldehyde/ketones and four acid catalysts are shown in Table 1.

The *mono*-ketals and 1,3-dioxane type ketal formations were not observed in any of the reactions. The only products observed are 1,3-dioxolane type *bis*-ketals and ketal-ethers with *cis*-2,4,7-trioxa [3.3.0] octane ring system. The cyclo-dehydration of 1,4-butanediol and *meso*-erythritol are known in acid catalyzed reactions [40]. In a recent study Takagaki has compared the cyclo-dehydration of erythritol using three Brønsted solid acids: HNbMoO₆, H-ZSM5 and Amberlyst-15. In this study HNbMoO₆ showed the highest activity for erythritol dehydration to 1,4-anhydroerythritol [40]. The only aldehyde used in our work, formaldehyde (**2a**) gave a mixtures of *bis*-acetal (**3a**) and *cis*-2,4,7-trioxa [3.3.0] octane (**4a**) with all homogeneous and heterogeneous catalysts tested. The best selectivity was found with the solid acid Amberlyst-15, which gave a mixture with 83% *cis*-2,4,7-trioxa [3.3.0] octane and only 17% of *bis*-acetal. Out of the three acyclic ketones **2b**, **c** and **d**, acetone showed 100% selectivity towards the

bis-ketal with homogeneous catalysts; whereas the use of heterogeneous catalyst SiO₂-SO₃H gave only the cyclo-dehydration product *cis*-3,3-dimethyl-2,4,7-trioxa [3.3.0] octane. In comparison, acyclic ketones in reactions using homogeneous catalyst *p*-TsOH the percentage of *bis*-ketal decreases as: 100, 98 and 73 as the size of alkyl group in the symmetrical ketone increases, indicating the sensitivity of the reaction to the size of the alkyl group. Similar trend can be found with homogeneous acidic ionic liquid catalyst as well; where *bis*-ketal percent decreases as: 100, 96 and 90 as the size of alkyl group increases. The preference towards the cyclo-dehydration of *meso*-erythritol under the heterogeneous catalysis conditions may be due to strong interactions of hydroxyl groups of *meso*-erythritol with multiple sulfonic acid groups on the surface of heterogeneous catalysts. Similar interactions between multiple hydroxyl and carboxylic acid groups are reported in the literature in carbohydrate systems [41]. In the case of 4-heptanone the change in homogenous catalyst from *p*-TsOH to Brønsted acidic ionic liquid $[(\text{HSO}_3)^3\text{C}_3\text{C}_1\text{im}][\text{Cl}]$ showed an improvement in selectivity towards the *bis*-ketal product and this type of selectivity as well as reaction product changes are known in the use of acidic ionic liquids in place of classical homogeneous acid catalysts [42]. The three cyclic ketones **2e–g** exclusively gave the *bis*-ketal products **3e–g** with all catalysts tested. This is probably due to lower steric hindrance around the carbonyl group in cyclic ketones when compared to acyclic ketones as methylene groups held are away from C=O forming the ring. The poor selectivity observed with the only aldehyde used in the study, formaldehyde may be due to kinetic reasons. The reactive small aldehyde may react faster than ketones giving different product distributions and this is particularly noted when cyclic ketones are used, where only bis ketals are formed.

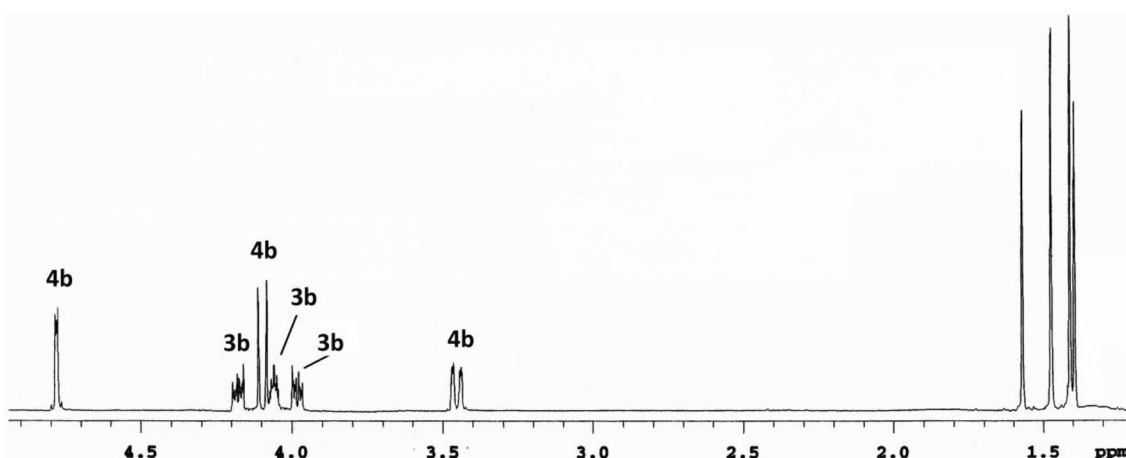


Fig. 3 The representative ^1H NMR of a sample of Amberlyst-15 H^+ catalyzed reaction of *meso*-erythritol (**1**) with acetone (**2b**) giving a mixture of **3b** and **4b**. *meso*-Erythritol (2.0 mmol), acetone

(6.0 mmol), Amberlyst-15 H^+ (0.094 mmol H^+) and 20 mL benzene, reflux using Dean-Stark water separator, 24 h

Table 1 The aldehyde/ketone used, catalyst, product yield (%) and composition (%) in the *p*-toluenesulfonic acid (*p*-TsOH), 1-(3-propylsulfonic)-3-methylimidazolium chloride $[(\text{HSO}_3)^3\text{C}_3\text{C}_1\text{im}][\text{Cl}]$, Amberlyst-15 H^+ and sulfonated-silica ($\text{SiO}_2\text{--SO}_3\text{H}$) catalyzed reactions of *meso*-erythritol (**1**) with aldehyde/ketone compounds (**2a–g**)

Entry	Aldehyde/ketone	Catalyst	Yield (%)	Composition (%)	
				3	4
1	Formaldehyde (2a)	<i>p</i> -TsOH	88	69	31
2		$[(\text{HSO}_3)^3\text{C}_3\text{C}_1\text{im}][\text{Cl}]$	84	43	57
3		Amberlyst-15	90	17	83
4		$\text{SiO}_2\text{--SO}_3\text{H}$	87	67	33
5	Acetone (2b)	<i>p</i> -TsOH	95	100	–
6		$[(\text{HSO}_3)^3\text{C}_3\text{C}_1\text{im}][\text{Cl}]$	92	100	–
7	3-Pentanone (2c)	Amberlyst-15	96	56	44
8		$\text{SiO}_2\text{--SO}_3\text{H}$	94	–	100
9		<i>p</i> -TsOH	97	98	2
10		$[(\text{HSO}_3)^3\text{C}_3\text{C}_1\text{im}][\text{Cl}]$	95	96	4
11	4-Heptanone (2d)	Amberlyst-15	98	46	54
12		$\text{SiO}_2\text{--SO}_3\text{H}$	92	–	100
13		<i>p</i> -TsOH	91	73	27
14		$[(\text{HSO}_3)^3\text{C}_3\text{C}_1\text{im}][\text{Cl}]$	94	90	10
15	Cyclopentanone (2e)	Amberlyst-15	93	2	98
16		$\text{SiO}_2\text{--SO}_3\text{H}$	97	8	91
17		<i>p</i> -TsOH	90	100	–
18		$[(\text{HSO}_3)^3\text{C}_3\text{C}_1\text{im}][\text{Cl}]$	85	100	–
19	Cyclohexanone (2f)	Amberlyst-15	84	100	–
20		$\text{SiO}_2\text{--SO}_3\text{H}$	82	100	–
21		<i>p</i> -TsOH	93	100	–
22		$[(\text{HSO}_3)^3\text{C}_3\text{C}_1\text{im}][\text{Cl}]$	90	100	–
23	Cycloheptanone (2g)	Amberlyst-15	95	100	–
24		$\text{SiO}_2\text{--SO}_3\text{H}$	92	100	–
25		<i>p</i> -TsOH	83	100	–
26		$[(\text{HSO}_3)^3\text{C}_3\text{C}_1\text{im}][\text{Cl}]$	87	100	–
27	<i>meso</i> -Erythritol (1)	Amberlyst-15	91	100	–
28		$\text{SiO}_2\text{--SO}_3\text{H}$	90	100	–

We have studied the reuse of four acid catalysts: *p*-toluene sulfonic acid (*p*-TsOH), 1-(3-propylsulfonic)-3-methylimidazolium chloride $[(\text{HSO}_3)^3\text{C}_3\text{C}_1\text{im}][\text{Cl}]$, Amberlyst-15 H^+ and sulfonated-silica. The reaction of *meso*-erythritol with cyclohexanone was selected for this study and all four catalysts gave only the *bis*-ketal product with the cyclic ketones, and the recovered catalyst was used for three more additional cycles in these experiments. The results

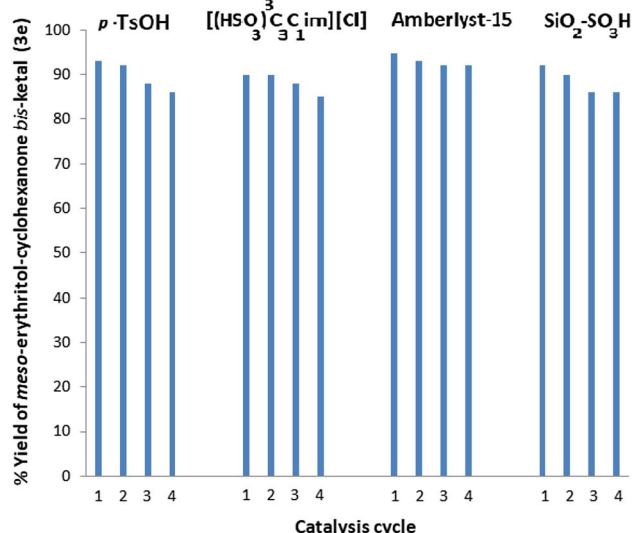


Fig. 4 The percent yields of *meso*-erythritol-cyclohexanone *bis*-ketal (**3f**) produced in reusing *p*-toluenesulfonic acid (*p*-TsOH), 1-(3-propylsulfonic)-3-methylimidazolium chloride $[(\text{HSO}_3)^3\text{C}_3\text{C}_1\text{im}][\text{Cl}]$, Amberlyst-15 H^+ and $\text{SiO}_2\text{--SO}_3\text{H}$ catalysts in the reaction of *meso*-Erythritol:cyclohexanone 1:3 in benzene under Dean-Stark conditions for 24 h, in all experiments

of reusing the catalyst are shown in Fig. 4. All four catalysts could be reused without significant loss in catalytic activity and the solid acid Amberlyst-15 showed the best recyclability as this catalyst is easy to recover by decantation and showed the minimum loss in activity after four cycles.

The proposed mechanism for formation of *cis*-2,4,7-trioxa [3.3.0] octane ring system in the acid catalyzed condensation reaction of *meso*-erythritol with aldehyde/ketones is shown in Fig. 5. First the protonation of a primary -OH group and intramolecular etherification gives the tetrahydrofuran ring, then a nucleophilic attack of -OH on a protonated carbonyl gives the next intermediate product. Since only a *cis* fusion is possible in a bicyclo [3.3.0] octane system, the 1,3-dioxolane ring closure occurs only by the protonation of the secondary -OH attached to the tetrahydrofuran ring. Finally, the S_N2 type nucleophilic attack with inversion gives the *cis* fused bicyclic ring system in **4**.

The Hartree–Fock (HF) calculations were performed to identify energetically most stable product from the reaction of *meso*-erythritol with the aldehydes and the ketones. In all cases, the calculations show that the *bis*-ketals products (**3**) are thermodynamically more stable than the ether products (**4**). In reactions using acyclic carbonyl compounds (a–d), the total energy of the products increased with the increase in the number of carbons and the difference in energy between product **3** and **4** (ΔE) also increased with the number of carbon atoms (Table 2). With

Fig. 5 The proposed mechanism for formation of the *cis*-2,4,7-trioxa [3.3.0] octane ring system (**4**) in acid catalyzed reactions of *meso*-erythritol with aldehyde/ketones

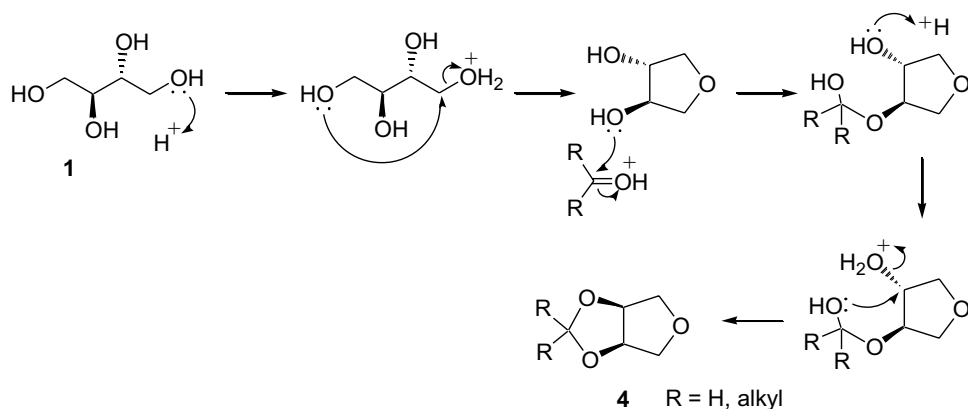


Table 2 The RHF 3-21G level calculated total energies of *bis*-ketal (**3**) (E_3), 1,3-dioxolane-ether (**4**) (E_4) products and energy differences (ΔE) in Hartree for Brønsted acid catalyzed reactions of *meso*-erythritol with aldehyde/ketones (**2a–g**)

Aldehyde/ketone	E_3	E_4	$\Delta E (E_3 - E_4)$
Formaldehyde (2a)	-529.49	-416.19	-113.30
Acetone (2b)	-684.80	-493.85	-190.95
3-Pentanone (2c)	-840.08	-571.49	-268.59
4-Heptanone (2d)	-995.35	-649.12	-346.23
Cyclopentanone (2e)	-837.73	-570.29	-267.44
Cyclohexanone (2f)	-940.40	-609.10	-331.30
Cycloheptanone (2g)	-993.03	-647.96	-345.07

acyclic ketone reactions, the homogeneous acid catalyzed reactions always gave the *bis*-ketal product as the major product, however with heterogeneous solid acid catalysts like $\text{SiO}_2\text{-SO}_3\text{H}$, the ether product was formed as the major product, probably due to the steric effects of larger alkyl groups in the acyclic ketones.

2.1 X-Ray structure of 2,2'-bi-1,4-dioxaspiro[4.5]decane, (R^*, S^*) (**3f**)

The X-ray structure of *meso*-erythritol-cyclohexanone *bis* ketal, 2,2'-bi-1,4-dioxaspiro[4.5]decane, (R^*, S^*) (**3f**) is shown in Fig. 6. The crystal packing of **3f** and geometric data (bond distances, bond angles and torsion angles) are presented in supplementary material. In the crystal structure the two dioxolane rings are positioned on the opposite sides of the central bond forming a linear molecule which allows the preparation of linear polymer chains via *bis*-ketal formation reactions. The resulting linear polymer chains may also be arranged in an ordered packed structure similar to the crystal packing structure of **3f** (electronic supplementary material). Therefore, the *bis*-ketal formation using cyclic ketones could be a good polymerization technique for the application of erythritol as a renewable polymer building block.

3 Conclusion

The ketalization and 1,3-dioxolane ether formation are competing reactions in acid catalyzed condensations of *meso*-erythritol with aldehydes and ketones. In the reaction using *para*-formaldehyde gave mixtures of *bis*-ketals and *cis*-2,4,7-trioxa [3.3.0] octane with all homogeneous and heterogeneous acid catalysts studied. We have found that excellent selectivity among *bis*-ketal and 1,3-dioxolane ether formation can be achieved in reactions with acyclic symmetrical ketones by choosing between homogeneous and heterogeneous catalysts. For instance, homogeneous acid catalysts *p*-toluenesulfonic acid and 1-(3-propylsulfonic)-3-methylimidazolium chloride gave *meso*-erythritol-acetone *bis*-ketal as the sole product in 95 and 92% yields respectively. On the other hand the reaction using the heterogeneous catalyst sulfonated-silica gave the 1,3-dioxolane ether product: *cis*-3,3-dimethyl-2,4,7-trioxa [3.3.0] octane as the sole product in 94% yield under similar catalyst loading and reaction conditions. As far as we are aware this is the first example of achieving a complete selectivity among ketal and ether formation processes in Brønsted acid catalyzed reaction between a polyol and ketones.

4 Experimental

4.1 Materials and instrumentation

meso-Erythritol (> 99%), paraformaldehyde (> 99%), acetone (> 99%), 3-pentanone (> 99%), 4-heptanone (> 99%), cyclopentanone (> 99%), cyclohexanone (> 99%), cycloheptanone (> 99%), *p*-toluenesulfonic acid monohydrate (99%), Amberlyst-15 hydrogen form (4.7 mequiv./g by dry weight), 1-methylimidazole (99%), 1,3-propanesultone (99%) and anhydrous benzene were purchased from Aldrich Chemical Co. Milwaukee, USA. The Brønsted acidic ionic liquid catalyst,

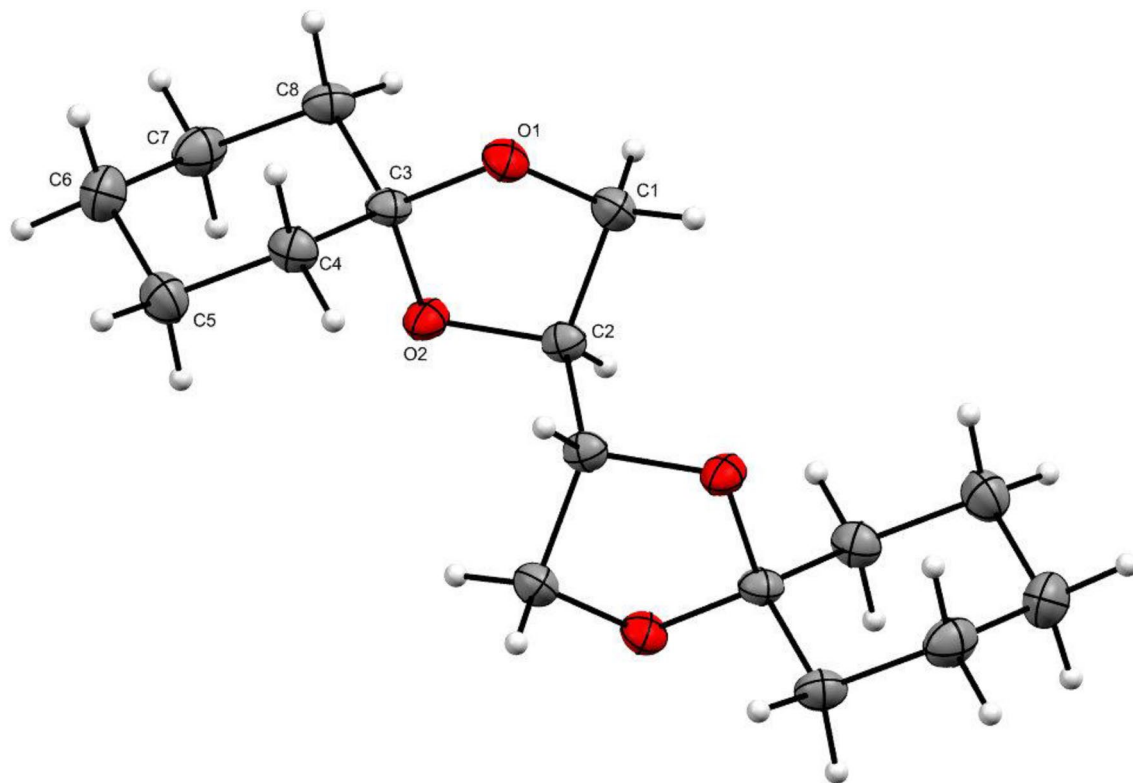


Fig. 6 Molecular structure of 2,2'-bi-1,4-dioxaspiro[4.5]decane (*R*, *S*) **3f** obtained by single crystal X-ray diffraction. Ellipsoids are presented at 50% probability. The crystal packing structure and geo-

metric parameters are given in the electronic supplementary material. Crystallographic data for **3f** is available from the Cambridge Crystallographic Data Center, CCDC 1845662

1-(3-propylsulfonic)-3-methylimidazolium chloride was prepared by condensation of 1,3-propanesultone and 1-methylimidazole and then treatment of the imidazolium zwitterion with HCl as shown in Fig. 2, following the literature procedure [33, 34, 43]. Sulfonated-silica ($\text{SiO}_2\text{--SO}_3\text{H}$) was prepared by using the standard published procedure [44, 45]. The acid group density in $\text{SiO}_2\text{--SO}_3\text{H}$ was determined as 2.52 mmol/g by titration with aq. NaOH (5.05×10^{-2} M) and using phenolphthalein as the indicator. The proton nuclear magnetic resonance spectra were recorded in chloroform-*d* (99%) on a 400 MHz Varian Mercury plus spectrometer and chemical shifts are given in ppm downfield from TMS ($\delta = 0.00$). The carbon NMR were recorded in the same spectrometer at 100 MHz, and chemical shifts were measured relative to chloroform-*d* and converted to δ (TMS) using δ (CDCl_3) = 77.00.

4.2 General procedure for the acid catalyzed ketalization of meso-erythritol with carbonyl compounds

A mixture of *meso*-erythritol (244 mg, 2.0 mmol), aldehyde/ketone (6.0 mmol), acid catalyst (*p*-toluenesulfonic acid, 1-(3-propylsulfonic)-3-methylimidazolium

chloride, Amberlyst-15 H^+ or $\text{SiO}_2\text{--SO}_3\text{H}$; 0.094 mmol H^+) in 20.0 mL of benzene was heated under reflux in a Dean-Stark apparatus for 24 h. Then samples with *p*-toluenesulfonic acid or 1-(3-propylsulfonic)-3-methylimidazolium chloride as the catalyst were washed with water (3×5 mL) and concentrated under reduced pressure. The concentrated product was weighed to measure the total product mass and analyzed by NMR spectroscopy. The samples with solid acid catalysts: Amberlyst-15 H^+ or $\text{SiO}_2\text{--SO}_3\text{H}$ were decanted to remove the catalyst, concentrated, weighed and similarly analyzed by NMR spectroscopy. The percent composition of the two products was calculated by using proton NMR peak areas corresponding to 2H's and the formula:

mole %bis-ketal (**3b**)

$$= \frac{\text{peak area at } 4.17 \text{ ppm}}{\text{peak area at } 4.17 \text{ ppm} + \text{peak area at } 4.78 \text{ ppm}} \times 100 \%$$

mole %ketal-ether (**4b**) = 100 – mole %bis-ketal (**3b**)

Similar equations were used in the calculation of bis-ketal (**3**), ketal-ether (**4**) product compositions in the

reactions carried out with other aldehyde/ketones and acid catalysts. The results are shown in Table 1.

The % yield was calculated using the formula: % yield = (moles of products) \times 100/(moles of *meso*-erythritol).

4.3 Computational study

The geometry optimizations and total energy calculations were carried out at 3-21G level. When R was substituted with different alkyl/cyclic groups, in order to obtain the optimized structures of the products (**3** and **4**), the heavy atoms, hydrogen atoms, bond lengths and all angles of the first structure was kept constant while optimizing all substituent bond lengths as well as angles. The computational work was performed using GAUSSIAN 16 W program [46] on an Intel (R) Core (TM) i7-3740QM CPU @ 2.70 GHz, 8.0 GB RAM 32 bit operating system. The total energies of *bis*-ketal **3** (E_3), 1,3-dioxolane-ether **4** (E_4) products and energy differences (ΔE) are listed in Table 2.

4.4 General procedure for the reuse of acid catalysts in ketalization of *meso*-erythritol with cyclohexanone

The reactions using cyclohexanone were carried out according to the general procedure 2.2. In homogeneous catalyst reactions the catalysts were recovered by evaporation of the combined aqueous phase. In reactions using heterogeneous catalysts, the catalysts were recovered by decanting the organic phase. The recovered catalyst was reused in three subsequent catalytic cycles and the percentage yields in reuse experiments are given in Fig. 4.

4.5 X-Ray structure determination of **3f**

The crystals of *meso*-erythritol cyclohexanone bis-ketal product (**3f**) were obtained by slow evaporation of a concentrated methanol solution at room temperature over 3 days, M.pt. 90–91 °C (Lit. 89–90 °C [37]). The crystal of **3f** ($C_{16}H_{20}O_4$, $M=282.37$) is orthorhombic, space group Pbca, at $T=100$ K: $a=8.3505(18)$ Å, $b=7.5675(17)$ Å, $c=23.461(5)$ Å, α , β , $\gamma=90^\circ$, $V=1482.6(6)$ Å³, $Z=4$, $d_{\text{calc}}=1.265$ g/cm³, $F(000)=616$, $\mu=0.089$ mm⁻¹. 22,612 total reflections (2556 unique reflections) were measured on a three-circle Bruker APEX-II CCD diffractometer ($\lambda(MoK_\alpha)$ -radiation, graphite monochromator, φ and ω scan mode, $2\theta_{\text{max}}=64.4^\circ$) and corrected for absorption ($T_{\text{min}}=0.661$; $T_{\text{max}}=0.746$) [47]. The structure was determined by direct methods and refined by full-matrix least squares technique on F^2 with anisotropic displacement parameters for non-hydrogen atoms. Hydrogen atoms were placed in calculated positions and refined within a

riding model with fixed isotropic displacement parameters [$U_{\text{iso}}(\text{H})=1.5U_{\text{eq}}(\text{C})$ for the CH_3 -groups and $1.2U_{\text{eq}}(\text{C})$ for the other groups]. The final divergence factors were $R_1=0.0409$ for 1983 independent reflections with $l>2\sigma(l)$ and $wR_2=0.1007$ for all independent reflections, $S=1.043$. All calculations were carried out using the SHELXTL program [48]. The X-ray structure of *meso*-erythritol - cyclohexanone bis ketal, 2,2'-bi-1,4-dioxaspiro[4.5]decane, (R^*,S^*) (**3f**) is shown in Fig. 6 and the crystal packing structure and geometric parameters are given in the electronic supplementary material. The crystallographic data for **3f** have been deposited with the Cambridge Crystallographic Data Center with deposition number CCDC 1845662.

Acknowledgements The authors would like to thank the National Science Foundation of the United States (NSF) (through Grant Nos. HRD-1036593, CBET-1336469, and DMR-1523611) for financial support.

Compliance with ethical standards

Conflict of interest The authors declare that they have no conflict of interest.

References

1. Wuts PG, Greene TW (2006) Greene's protective groups in organic synthesis. Wiley, New York
2. Ma S, Webster DC (2018) Degradable thermosets based on labile bonds or linkages: a review. *Prog Polym Sci* 76:65–110
3. Trifoi AR, Agachi PŞ, Pap T (2016) Glycerol acetals and ketals as possible diesel additives. A review of their synthesis protocols. *Renew Sustain Energy Rev* 62:804–814
4. Morinaga H, Morikawa H, Endo T (2018) Controlled release of fragrance with cross-linked polymers: synthesis and hydrolytic property of cross-linked amphiphilic copolymers bearing octanal-derived acetal moieties. *Polym Bull* 75:197–207
5. Chen D, Wang H (2014) Novel pH-sensitive biodegradable polymeric drug delivery systems based on ketal polymers. *J Nanosci Nanotechnol* 14:983–989
6. Louage B, Zhang Q, Vanparijs N, Voorhaar L, Vande Castele S, Shi Y, Hennink WE, Van Boclaer J, Hoogenboom R, De Geest BG (2014) Degradable ketal-based block copolymer nanoparticles for anticancer drug delivery: a systematic evaluation. *Biomacromolecules* 16(1):336–350
7. Rostagno M, Price EJ, Pemba AG, Ghiriviga I, Abboud KA, Miller SA (2016) Sustainable polyacetals from erythritol and bioaromatics. *J Appl Polym Sci* 133(45):44089–44093
8. Pemba AG, Rostagno M, Lee TA, Miller SA (2014) Cyclic and spirocyclic polyacetal ethers from lignin-based aromatics. *Polym Chem* 5(9):3214–3221
9. Freitas FA, Licursi D, Lachter ER, Galletti AMR, Antonetti C, Brito TC, Nascimento RSV (2016) Heterogeneous catalysis for the ketolisation of ethyl levulinate with 1,2-dodecanediol: opening the way to a new class of bio-degradable surfactants. *Catal Commun* 73:84–87
10. Mullen BD, Badarinayana V, Santos-Martinez M, Selifonov S (2010) Catalytic selectivity of ketalization versus transesterification. *Topics Catal* 53(15–18):1235–1240

11. Shenoi RA, Abbina S, Kizhakkedathu JN (2016) In vivo biological evaluation of high molecular weight multifunctional acid-degradable polymeric drug carriers with structurally different ketals. *Biomacromolecules* 17:3683–3693
12. Nanda MR, Yuan Z, Qin W, Ghaziskar HS, Poirier M-A, Xu C (2014) Catalytic conversion of glycerol to oxygenated fuel additive in a continuous flow reactor: process optimization. *Fuel* 128:113–119
13. Esteban J, Murasiewicz H, Simons TAH, Bakalis S, Fryer PJ (2016) Measuring the density, viscosity, surface tension, and refractive index of binary mixtures of cetane with solketal, a novel fuel additive. *Energy Fuels* 30:7452–7459
14. Amarasekara AS, Hawkins SA (2011) Synthesis of levulinic acid-glycerol ketal-ester oligomers and structural characterization using NMR spectroscopy. *Eur Polym J* 47(12):2451–2457
15. Amarasekara AS, Hasan MA, Larkin E (2017) Renewable polymers: synthesis and characterization of poly (4-ketopimelic acid-glycerol). *J Renew Mater* 5(1):62–66
16. Amarasekara AS, Razzaq A, Bonham P (2013) Synthesis and characterization of all renewable resources based branched polyester: poly (2,5-furandicarboxylic acid-co-glycerol). *ISRN Polym Sci* 2013:645169
17. Bueno M, Molina I, Galbis JA (2012) Degradable “click” polyesters from erythritol having free hydroxyl groups. *Polym Degrad Stab* 97:1662–1670
18. Barrett DG, Luo W, Yousaf MN (2010) Aliphatic polyester elastomers derived from erythritol and α , ω -diacids. *Polym Chem* 1(3):296–302
19. Moon H-J, Jeya M, Kim I-W, Lee J-K (2010) Biotechnological production of erythritol and its applications. *Appl Microbiol Biotechnol* 86(4):1017–1025
20. Nelson RT (1951) Hydrogenation of tartaric acid esters to erythritol. US Patents, US2571967A
21. Sloan JW, Hofreiter BT, Mchltretter CL, Wolff IA (1957) Hydrogenolysis of dialdehyde starch to erythritol and ethylene glycol. US Patent US 2,783,283
22. Stapley JA, Genders JD, Atherton DM, Kendall PM (2011) Methods for the electrolytic production of erythrose or erythritol. US Patents, US7955489B2
23. Rzchonek DA, Dobrowolski A, Rymowicz W, Mirończuk AM (2018) Recent advances in biological production of erythritol. *Critical Rev Biotechnol* 38(4):620–633
24. Ozbay N, Oktar N, Dogu G, Dogu T (2013) Activity comparison of different solid acid catalysts in etherification of glycerol with *tert*-butyl alcohol in flow and batch reactors. *Topics Catal* 56:1790–1803
25. Wilson P, Kaliya ML, Landau MV, Herskowitz M (2004) Catalytic acetylation of aromatics with metal chlorides and solid acids—a comparative study. *Eurasian Chem Technol* 6:193–199
26. Yoon JW, Jhung SH, Chang J-S (2008) Trimerization of isobutene over solid acid catalysts: comparison between cation-exchange resin and zeolite catalysts. *Bull Korean Chem Soc* 29:339–341
27. Amarasekara AS, Animashau MA (2016) Acid catalyzed competitive esterification and ketalization of levulinic acid with 1, 2 and 1, 3-diols: the effect of heterogeneous and homogeneous catalysts. *Catal Lett* 146(9):1819–1824
28. Amarasekara AS, Ha U, Okorie NC (2018) Renewable polymers: synthesis and characterization of poly(levulinic acid-pentaerythritol). *J Polym Sci Part A Polym Chem* 56:955–958
29. Amarasekara AS, Singh TB, Larkin E, Hasan MA, Fan H-J (2015) NaOH catalyzed condensation reactions between levulinic acid and biomass derived furan-aldehydes in water. *Ind Crops Prod* 65:546–549
30. Amarasekara AS, Hasan MA (2015) Pd/C catalyzed conversion of levulinic acid to γ -valerolactone using alcohol as a hydrogen donor under microwave conditions. *Catal Commun* 60:5–7
31. Amarasekara AS, Razzaq A (2012) Vanillin-based polymers—part II: synthesis of Schiff base polymers of vanillin and their chelation with metal ions. *ISRN Polym Sci* 2012:532171–532176
32. Amarasekara AS, Green D, Williams LD (2009) Renewable resources based polymers: synthesis and characterization of 2,5-diformylfuran-urea resin. *Eur Polym J* 45(2):595–598
33. Gui J, Cong X, Liu D, Zhang X, Hu Z, Sun Z (2004) Novel Brønsted acidic ionic liquid as efficient and reusable catalyst system for esterification. *Catal Commun* 5(9):473–477
34. Yang Q, Wei Z, Xing H, Ren Q (2008) Brønsted acidic ionic liquids as novel catalysts for the hydrolysis of soybean isoflavone glycosides. *Catal Commun* 9(6):1307–1311
35. Nouguier R, Gras J-L, Mchlich M (1988) Re’ activite’ dume’ so-erythritol et du thre’ itol visavis de la reaction de transacetalisation par le dime’ thoxyme’ thane. *Tetrahedron* 44(10):2943–2950
36. Aslani-Shotorbani G, Buchanan JG, Edgar AR, Henderson D, Shavidi P (1980) Application of ^{13}C NMR in a re-examination of the isopropylideneation of D-ribose diethyldithioacetal and erythritol. *Tetrahedron Lett* 21(18):1791–1792
37. Annunziata R, Cinquini M, Cozzi F, Raimondi L, Stefanelli S (1986) Stereoselective synthesis of polyols precursors by allyl sulphinyl anion addition to chiral alkoxy aldehydes. *Tetrahedron* 42(19):5451–5456
38. Buchanan JG, Edgar AR, Rawson DL, Shahidi P, Wightman RH (1982) Assignment of ring size in isopropylidene acetals by carbon-13 nmr spectroscopy. *Carbohydr Res* 100(1):75–86
39. Awal A, Boyd AS, Buchanan JG, Edgar AR (1990) The formation of isopropylidene acetals of erythritol and ribitol under conditions of kinetic control. *Carbohydr Res* 205:173–179
40. Takagaki A (2016) Kinetic analysis of aqueous-phase cyclodehydration of 1,4-butanediol and erythritol over a layered niobium molybdate solid acid. *Catal Sci Technol* 6(3):791–799
41. Kobayashi H, Yabushita M, J-y Hasegawa, Fukuoka A (2015) Synergy of vicinal oxygenated groups of catalysts for hydrolysis of cellulosic molecules. *J Phys Chem C* 119(36):20993–20999
42. Amarasekara AS, Okorie NC (2018) 1-(Alkylsulfonic)-3-methylimidazolium chloride Brønsted acidic ionic liquid catalyzed hydrogen peroxide oxidations of biomass derived furan aldehydes. *Catal Commun* 108:108–112
43. Amarasekara AS (2016) Acidic ionic liquids. *Chem Rev* 116(10):6133–6183
44. Shaterian HR, Ghashang M, Feyzi M (2008) Silica sulfuric acid as an efficient catalyst for the preparation of 2H-indazolo [2, 1-b] phthalazine-triones. *Appl Catal A Gen* 345(2):128–133
45. Amarasekara AS, Owereh OS (2010) Synthesis of a sulfonic acid functionalized acidic ionic liquid modified silica catalyst and applications in the hydrolysis of cellulose. *Catal Commun* 11(13):1072–1075
46. Frisch M, Trucks G, Schlegel H, Scuseria Gw, Robb M, Cheeseman J, Montgomery J, Vreven T, Kudin K, Burant J (2008) Gaussian 03, revision C. 02
47. Sheldrick GM (2003) SADABS, v. 2.03, Bruker/Siemens area detector absorption correction program; Bruker AXS Inc., Madison
48. Sheldrick GM (2008) A short history of SHELX. *Acta Crystallogr Sect A Found Crystallogr* 64(1):112–122